## 2. TOKAMAK ISTTOK

C.A.F. Varandas (Head), H. Fernandes and C. Silva (Deputy Heads), A. Soares, A. Vannucci, B.B. Carvalho, D. Valcárcel, I. Carvalho, I. Nedzelskij, M.P. Alonso, P. Carvalho, R. Coelho, H. Figueiredo, J. Figueiredo, J. Fortunato, R. Gomes, A. Neto, T. Pereira, V. Plyusnin, Y. Tashchev

### 2.1. INTRODUCTION

ISTTOK is a small-size (R=46 cm, a=8.5 cm), large aspect-ratio, low magnetic field (0.46 T) limiter tokamak with an iron core transformer (flux swing of 0.22 Vs), equipped with a distributed VME control and data acquisition system. Its low temperature (150 eV), low density ($8x10^{18}$ $m^{-3}$) plasmas are diagnosed by electric and magnetic probes, a microwave interferometer, a heavy ion beam diagnostic and spectroscopic diagnostics.

The main objectives of this project are: (i) development of new diagnostic and control and data acquisition systems; (ii) testing of new operation scenarios (liquid metal limiter and alternating plasma current); (iii) study of the influence of external applied signals on the plasma confinement and stability; and (iv) education and training on tokamak physics and engineering.

This project included in 2005 work in the following main research areas:

- Testing of the liquid metal limiter concept;
- Optimization of the ISTTOK operation;
- Diagnostics;
- Control and data acquisition;
- Plasma physics studies.

### 2.2. TESTING OF THE LIQUID METAL LIMITER CONCEPT[1]

IST/CFN has proceeded with the testing of the liquid metal limiter concept.

The *liquid metal loop experimental facility* has been successful filled with oxide-free Gallium. The overall setup has been tested showing satisfactory operation of the device.

The *jet stability and reproducibility* has been studied for the 2.30 mm diameter nozzle, which is planned to be used in the tokamak, since it produces a close to 13 cm continuous jet length. The time evolution for a 6 s main valve opening is shown in Figure 2.1. Gallium jet flow velocities and jet Break-Up Length parameter (BUL) have been measured for 1.45, 1.80, 2.09, 2.30 and 2.40 mm nozzle diameters. The results are presented in Figures 2.2 and 2.3.

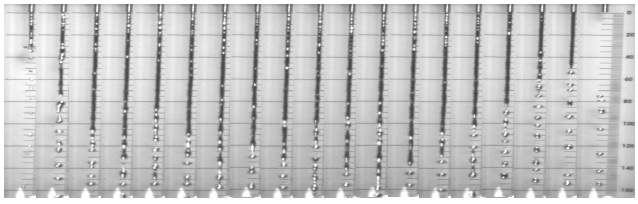

*Figure 2.1 - The gallium jet time evolution for a 6 s valve opening using a 2.30 mm nozzle. Each frame was obtained using a 700 μs exposition.*

The *influence of a pulsed magnetic field* (0.25 T, 60 ms) *on the jet characteristics* has been analysed for both spatially uniform line distribution and with a high gradient perturbation. Transients in the magnetic field were found not to perturb significantly the jet behaviour;

Finally, careful studies have been carried out on the observed *scattering of Gallium droplets* from the lower collector to the main chamber. A damping device has already been tested. Although it has shown a clear reduction on the number of large size (~ 0.5 to 0.2 mm) droplets, until now, it has been unsuccessful to fully eliminate the appearance of small (~10 to 200 μm size) ones. A more technically advanced damping device is under development in order to achieve a full elimination of the droplets that could reach the tokamak vessel.

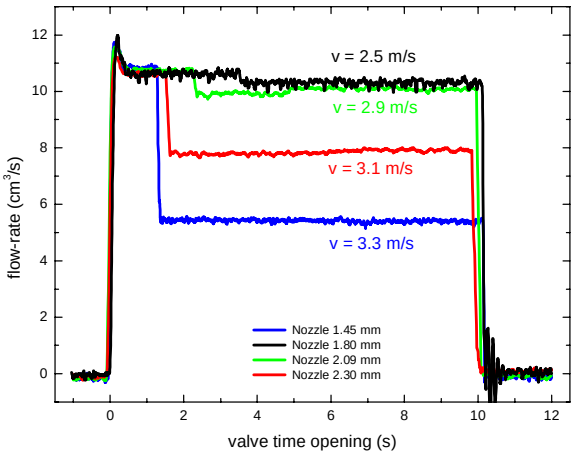


*Figure 2.2 - Flow rate and flow velocity for several nozzle sizes.*

[1] Work carried out in collaboration with the Association EURATOM/University of Latvia. Contact Person: O. Lielausis

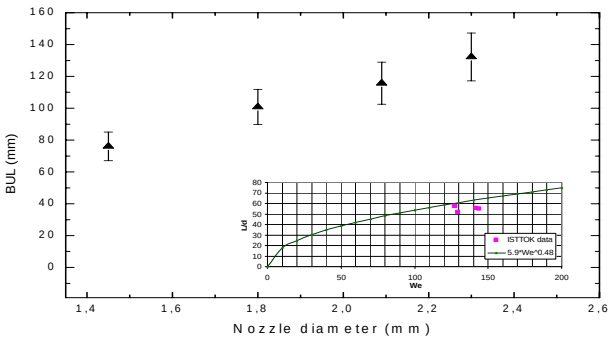


*Figure 2.3 - Break-up length (L) for several nozzle sizes and as a function of Weber number.*

## 2.3 OPTIMIZATION OF THE ISTTOK OPERATION

Aiming at optimizing the ISTTOK operation, the *gas injection system* has been upgrade by using a fast valve to allow a better control of the plasma density. The *RF generator* used for the discharge pre-ionization has been replaced by a *biased tungsten filament***.** The *new set of external coils* has been simultaneously used as the transformer primary and as a partial vertical field generator. This approach allows a smaller current on the vertical field quadrupole, with a much higher response time for feedback proposes.

## 2.4. DIAGNOSTICS

### 2.4.1. Main activities

This research line included activities on spectroscopy for the analysis of Gallium impurities[2], X-ray tomography, retarding field energy analyzer and emissive probes.

The *spectroscopy diagnostic*, designed to measure neutral Ga density on ISTTOK, has been improved by introducing a multi-channel (x8) fiber in order to acquire Ga spatial density profiles at the plasma edge. The required software has been modified and the diagnostic tested using tokamak cleaning discharges as a plasma source.

A *commercial, low cost, CCD video camera* has been tested. The test proved that these types of cameras are not adequate to be used as detectors in a soft X-ray tomography diagnostic due to the high noise level and the slow acquisition rate. A new diagnostic based on three linear 10-pixel detectors to perform real-time tomography from three different views has been designed.

The design, installation and testing of a *retarding field energy analyzer* for the measurement of the edge ion temperature has been performed.

An improved version of the *multi-pin array of emissive probes* has been installed on ISTTOK (Figure 2.4), which allows the simultaneous measurement of the density, poloidal and radial electric field, and their fluctuations in a spatial scale smaller than the turbulence correlation length.

### 2.4.2. Retarding Field Energy Analyzer

The retarding field energy analyzer (Figure 2.5) is rather compact (D14×L23 mm$^2$) and consits of an input 0.6 mm stainless steel pinhole (S), three Ni grids (G1, G2, G3) and a Cu collector plate (C) separated by MICA insulators. The grid stack is assembled in a boron nitride cup with a 14 mm of external diameter and with 2 mm diameter opening on the pinhole side.

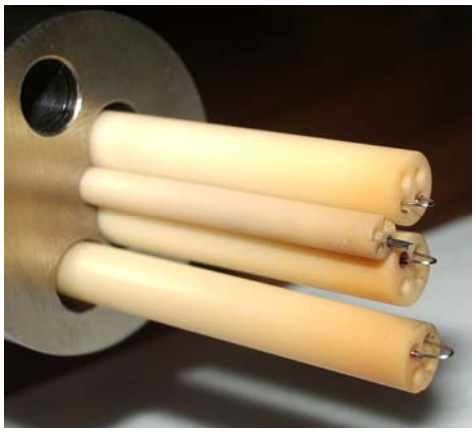

*Figure 2.4 - The ISTTOK probe system, consisting of three emissive probes and one cold probe.*

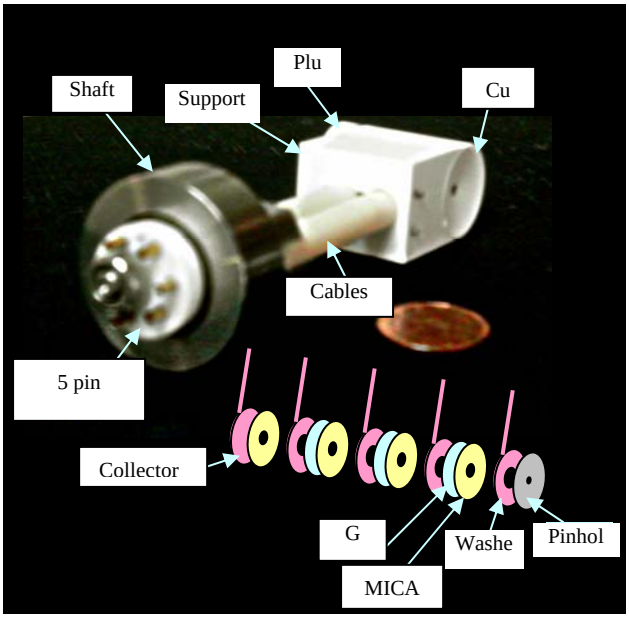


*Figure 2.5 - Photograph and schematically illustration of the retarding field energy analyser*

[2] Work carried out in collaboration with the Association EURATOM/University of Látvia. Contact Person: Ivars Tale.

A +100 V sawtooth voltage is applied to the second grid $G_2$ to obtain the ions characteristic, while grids $G_1$ and $G_3$ are kept at –50 V to suppress the respective electron flux from plasma and secondary electrons from collector. Figure 2.6 shows a typical characteristic obtained in the ISTTOK scrape-off layer (1.3 cm outside the limiter) as well as an exponential fit to the experimental data. The derived ion temperature ($T_i$ = 14 eV) is typically a factor of two larger than that of the electrons at the same location, which is in agreement with the results of the scrape-off layer models.

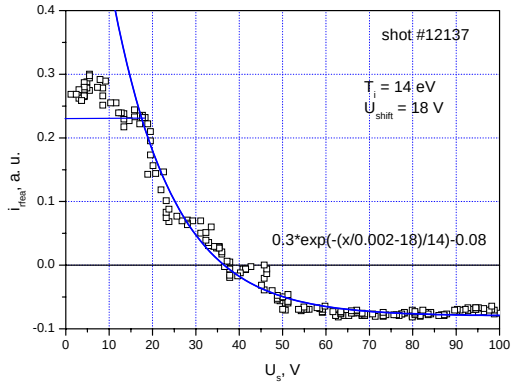


*Figure 2.6 - Typical characteristic obtained in the ISTTOK scrape-off layer*

## 2.5. CONTROL AND DATA ACQUISITION

### 2.5.1. Main activities

In 2005, a *real-time controller* for the horizontal plasma position, a *PCI timing board*, a new version of *software for shared remote data consulting and analysis* and *remote data analysis tools* have been developed. New *power supplies* have been designed and commissioned with optically isolated communication circuits and with local processing capabilities for self-implementation of control algorithms.

### 2.5.2. Real-time controller for the horizontal plasma position

The real-time controller for the horizontal plasma position allows controlling the vertical magnetic equilibrium field using a novel power supply. This controller is based on an existing PCI module (PCI-TR-256), developed at CFN.

The main technical characteristics of this module are:

- 8 galvanic isolated channels, with 14-bit ADC @ 2 MHz;
- a Texas Instruments Fixed-Point DSP @ 500 MHz (TMS320C6415);
- a Xillinx FPGA (Spartan-IIE XC2S400E);
- 512 MB SDRAM memory module;

The module software acquires data from 8 poloidal magnetic probes, removes the offset present in the signals, numerically integrates them, calculates the plasma position using the current filaments method and generates a power supply control signal with a PI controller. Off-line tests show that this system is capable of performing the plasma position calculation in 74 µs and that its time evolution is similar to the plasma position calculated offline with floating-point numerical codes running in MatLab.

### 2.5.3. Timing board

A new PCI-EPN board is intended to improve the trigger and the synchronism between the various ISTTOK diagnostics and allowing the migration of the ISTTOK CODAS to an event based system. The boards are on prototype stage and are planned to be operational earlier 2006.

### 2.5.4 New power supplies

A new concept of switched power supplies (57 kHz) were designed and completed with an embedded microcontroller, for the necessary current drive of the vertical and horizontal magnetic fields. This option allows a direct implementation of PID algorithms with a faster response time. Each power supply will allow a maximum current of 100A, with a very compact design and bipolar capabilities.

### 2.5.5. Cooperative software for shared tokamak operation

A new version of a multi-user platform, based on standards like CORBA, XML and JAVA, has been developed for remote control and data acquisition experiments. The main objective of this tool is to detach the machine operation from a single computer, allowing hardware configuration, experiment follow and data share by all the connected users. Among the main features it has a built-in chat, profile saving and sharing and remote calculation invocation. Since it was developed in JAVA and deployed with JAVA Web-Start technology, it can run in all the most common operating systems and computer platforms like PCs, Solaris and Mac in a very intuitive way. The software is plugin based, providing an easy way of adding new hardware, data viewers and data calculation algorithms. Since every hardware is described in a XML file, the program automatically creates configurators to the hardware. Every time a configuration is changed, the information is sent to hardware controller so that in the next discharge the hardware is programmed accordingly.

### 2.5.6. Remote data analysis tools

Based on the Extensible Markup Language (XML) and the Remote Method Invocation (RMI) standards, a client/server remote data analysis application has been developed for intensive data processing. This GRID oriented philosophy presents a powerful tool to maintain centralized computational resources (Figure 2.7). Another major feature is the ability to share proprietary algorithms in remote computers without the need of local code and

libraries installation and maintenance. The 16 CPU Orionte cluster in operation at CFN is currently used to provide remote data analysis. The codes running in languages such as Octave, C, Fortran or IDL are called through a script remote invocation and data is released to the client as soon as available. The remote calculations parameters are described in a XML file containing the configuration for the server runtime environment. Since the execution is made by calling a script any program can be launched to perform the analysis. Some properties of the ISTTOK plasma that require heavy computational resources are already obtained using this approach, allowing ready intershot analysis and parameterization decisions.

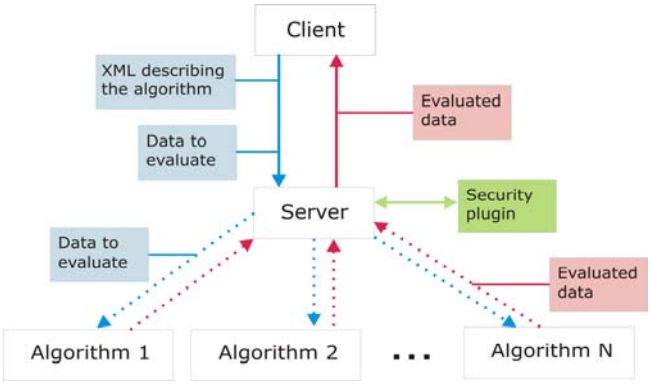


*Figure 2.7 - The remote data analysis protocol scheme*

## 2.6. PLASMA PHYSICS STUDIES

### 2.6.1. Introduction

The ISTTOK plasma physics studies were related in 2005 with:

- Control of edge transport by emissive electrode biasing;
- Plasma SOL flow measurements;
- Emissive probe measurements.

### 2.6.2. Control of edge turbulent transport by emissive electrode biasing

Emissive electrode biasing experiments have been previously investigated on ISTTOK. Experiments revealed that although a large radial electric field is induced by emissive electrode bias for both polarities (up to ±15 kV/m), a significant improvement in particle confinement is only observed for negative bias. The main motivation for this work is therefore to contribute to the better understanding of the distinct plasma behaviour with positive and negative bias. The boundary plasma was further characterized with focus on the relation between ExB sheared flows and particle transport. The use of emissive electrodes allowed, for the first time, the extension of this investigation to negative bias.

The ExB flow shear has been independently estimated from a radial array of Langmuir probes and a Gundestrup probe, which measures the parallel and perpendicular plasma flows. A good agreement has been found both in the profile and the absolute magnitude. We have observed that the magnitude of the ExB flow shear, in the region just inside the limiter position, is larger for negative bias. The ExB sheared flows induced by negative bias exceeds significantly the turbulence de-correlation time across most of the boundary plasma, while for positive bias this is only valid near the LCFS (r-a>-4 mm). The importance of the ExB flow shear on the global particle confinement has been demonstrated by the good correlation observed between these two quantities for both polarities in a wide range of bias conditions (Figure 2.8). We have found that above a certain threshold value of the ExB shearing rate (~$1x10^6$ kV/$m^2$) an improvement in particle confinement is observed for both polarities, being that value a factor of three larger than the turbulence de-correlation time. Results support therefore that the distinct particle confinement behaviour observed for positive and negative bias is related with the different ExB flow profile induced by edge biasing.

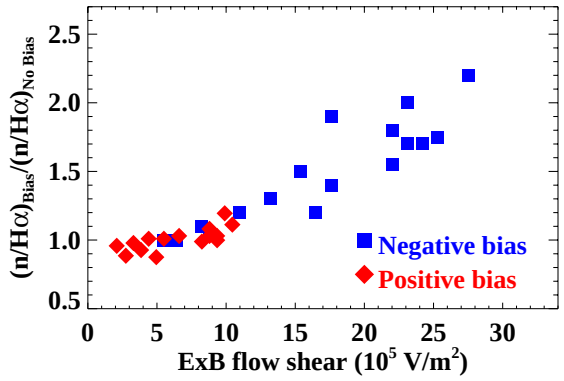


*Figure 2.8 - Dependence of the modification in particle confinement induced by electrode biasing ($[n/H_\alpha]_{Bias}/[n/H_\alpha]_{No\ Bias}$) with the ExB shearing rate in the region just inside the LCFS.*

The effect of electrode bias on the edge turbulent transport has also been investigated identifying the changes induced on the fluctuations frequency spectrum and probability distribution function, PDF. We have observed that negative electrode bias reduces the large amplitude, low frequency events, resulting in low amplitude fluctuations with a near Gaussian distribution across most of the scanned region. For positive bias, a substantial reduction of the fluctuations is also observed in the SOL. However, large amplitude, broad spectrum fluctuations appear in the core periphery, which increase the cross-field transport and contribute to the observed asymmetry in particle confinement with the bias polarity.

### 2.6.3. Plasma SOL flow measurements

Plasma SOL flow measurements were made using a Gundestrup Probe. A 1D fluid probe model was used to

deduce the parallel and perpendicular components of the unperturbed flow, taking into account the roundness of the collectors. The radial profile of the Mach numbers is shown in Figure 2.9. We note that the positive bias is not able to drive large sheared flows, which for both type of bias are larger around the limiter radius. The perpendicular Mach number behaves in opposite ways inside the LCFS and in the SOL region when bias is applied. We further note that the unbiased plasma exhibits a toroidal flow of about 0.2 throughout the measured region, being the direction the same as that of the toroidal field and plasma current. Furthermore, we note that the modification induced by biasing in the flows is maximum for negative bias and occurs in the region just inside the limiter for both parallel and perpendicular flows.

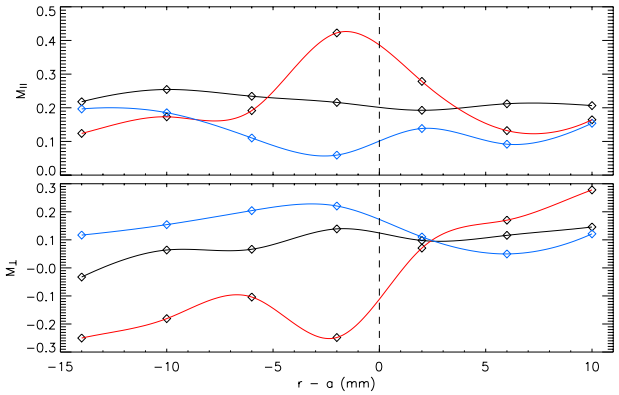


*Figure 2.9 - Radial traces of parallel and perpendicular Mach numbers.*

### 2.6.4. Emissive probe measurements[3]

Detailed measurements of the edge quantities with high temporal and radial resolutions have been performed with a multi-pin array of emissive probes. The main aim of this work was to investigate the importance of temperature fluctuations in the turbulent transport estimation. Both the root mean square of the poloidal electric field and the fluctuation-induced particle flux were found to be significantly larger when measured with the emissive probes, indicating that temperature fluctuations are important for the particle flux determination. The flux distribution was also found to be more peaked and asymmetric when measured with the emissive probes (Figure 2.10). A clear reduction of the turbulent particle flux and an improvement of the plasma confinement are observed during the negative emissive electrode biasing.

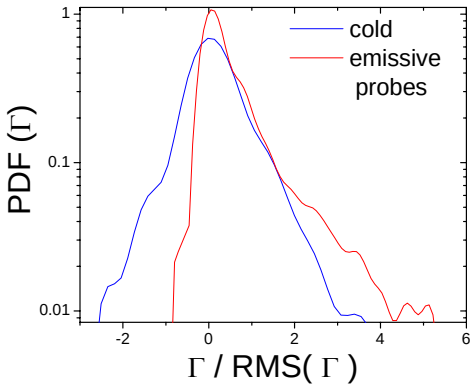


*Figure 2.10 - Probability distribution functions for the normalized turbulent particle flux at r = -8 mm inside LCFS.*

[3] Work carried out in collaboration with the Association EURATOM/OAW (University of Innsbruck). Contact Person: Roman Schrittwieser.